

## Nonequilibrium Energetics of Molecular Motor Kinesin

Takayuki Ariga,<sup>1,2,\*</sup> Michio Tomishige,<sup>3</sup> and Daisuke Mizuno<sup>2</sup>

<sup>1</sup>*Graduate School of Medicine, Yamaguchi University, Yamaguchi 755-8505, Japan*

<sup>2</sup>*Department of Physics, Kyushu University, Fukuoka 819-0395, Japan*

<sup>3</sup>*Department of Physics and Mathematics, Aoyama Gakuin University, Kanagawa 252-5258, Japan*

 (Received 18 April 2017; revised manuscript received 18 July 2018; published 21 November 2018)

Nonequilibrium energetics of single molecule translational motor kinesin was investigated by measuring heat dissipation from the violation of the fluctuation-response relation of a probe attached to the motor using optical tweezers. The sum of the dissipation and work did not amount to the input free energy change, indicating large hidden dissipation exists. Possible sources of the hidden dissipation were explored by analyzing the Langevin dynamics of the probe, which incorporates the two-state Markov stepper as a kinesin model. We conclude that internal dissipation is dominant.

DOI: [10.1103/PhysRevLett.121.218101](https://doi.org/10.1103/PhysRevLett.121.218101)

Kinesin-1 (hereafter called kinesin) is a molecular motor that transports various cargos along microtubules throughout the cell [1,2]. Single molecule kinesin takes 8 nm steps [3] per ATP hydrolysis [4,5] on a microtubule rail and generates  $\approx 7$  pN maximum force [6–8]. The two catalytic sites (heads) hydrolyze ATP in a “hand-over-hand” manner that mimics bipedal walking [9–11] by alternating its two heads in coordination with different nucleotide-microtubule binding states [12]. Kinesin shows backward steps occasionally at no load and frequently at high loads [13–15]. Recent experiments indicate that the biased unidirectional motion is achieved by regulating selective binding (unbinding) of the head to (from) the appropriate binding site [16–20]. Contrary to the molecular mechanism of the motility, the thermodynamic energetics of the motor is poorly understood due to kinesin’s stochastic and non-equilibrium behavior.

The energetics of single-molecule motors were historically discussed when their stall forces were measured [21]. Kinesin’s stall force of  $\approx 7$  pN indicates that maximum work per 8-nm step ( $\approx 56$  pN nm) is smaller than the physiological free energy change per ATP hydrolysis ( $\approx 85$  pN nm). This is in contrast to rotary motor F<sub>1</sub>-ATPase, whose stall force explains all input free energy [22]. Kinesin’s inefficient work at stall has been regarded as an “open problem” [23]. However, it may not be appropriate to evaluate kinesin efficiency from the stall force for two reasons. First, it is believed that kinesin consumes ATP at backsteps instead of synthesizing ATP [13–15], indicating that the stall condition is not thermodynamically (quasi-)static. Second, the physiological role of kinesin is to carry vesicles against viscous media, meaning that the input energy is dissipated as “heat” rather than “work.” Thus, measuring the “dissipation” from the motor is essential when discussing kinesin’s nonequilibrium energetics in physiologically relevant conditions.

The Harada-Sasa equality is best suited for this purpose [24,25]:

$$J_x = \gamma \bar{v}^2 + \gamma \int_{-\infty}^{\infty} [\tilde{C}(f) - 2k_B T \tilde{R}'(f)] df. \quad (1)$$

Here,  $J_x$  is total heat dissipation per unit time from the system through specific degrees of freedom (d.o.f.) indicated with subscript  $x$ .  $\gamma$  is viscous drag, and  $\bar{v} \equiv \langle \dot{x} \rangle$  is mean velocity, where  $\langle \cdot \rangle$  denotes the ensemble average.  $\tilde{C}(f)$ , with frequency  $f$ , is a Fourier transform of the correlation function of velocity fluctuations,  $C(t) \equiv \langle [v(t) - \bar{v}][v(0) - \bar{v}] \rangle$ .  $\tilde{R}(f)$  is a Fourier transform of the velocity response function, and the prime indicates the real part of the function.  $k_B$  is the Boltzmann constant, and  $T$  is the absolute temperature. It is known that the fluctuation-response relation (FRR),  $\tilde{C}(f) = 2k_B T \tilde{R}'(f)$ , is held in equilibrium [26], but the relation is violated in nonequilibrium conditions [27,28]. The integral in Eq. (1) thus indicates heat dissipation that appears only in nonequilibrium systems [29–32]. Since the formula is written with experimentally accessible quantities, Eq. (1) allows us to obtain nonequilibrium heat dissipation, which has been hard to measure directly in small stochastic systems.

Here, we measured the nonequilibrium energy flow of single-molecule walking kinesin via the FRR violation of an attached probe particle using optical tweezers. By analyzing the energy transmission between the probe and kinesin molecule with a mathematical kinesin model, we conclude that the unidirectional motion of kinesin consumes its chemical energy mainly as internal dissipations.

The experimental setup was based on the microscope equipped with optical tweezers described in Refs. [33,34] with modifications to incorporate a fast feedback force clamp and epi-fluorescent imaging [Fig. 1(a); see also

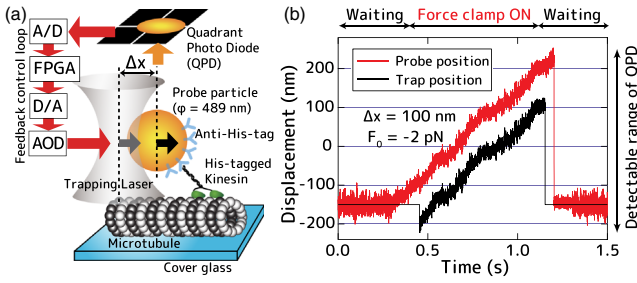


FIG. 1. (a) Schematic of the experimental setup for force clamp measurement of kinesin movement (not to scale). (b) Typical trace of probe (red) and trap (black) position with the FPGA force clamp. Both sampling and feedback rates are 20 kHz. Trap stiffness is 0.02 pN/nm.

Ref. [35] for details]. Tail-truncated kinesin constructs [12,35,36] were conjugated to 489 nm probe particles [35,37]. Fluorescent microtubules [35,38] were nonspecifically attached to a glass flow cell. After the cell was washed with casein solution, the probes were trapped on the microtubule at the indicated concentrations of ATP, ADP and potassium phosphate ( $P_i$ ) at  $25 \pm 1^\circ\text{C}$ . The bright field image of the trapped probe was projected onto quadrant photodiodes (QPD), and the signals were acquired by a field programmable gate array (FPGA)-embedded data acquisition board at a sampling rate of 20 kHz. The feedback-regulated trap positions were calculated from the signals on the FPGA circuit at the same rate, allowing the probe to apply arbitrary force via acousto-optic deflectors (AOD). Displacement calibration was performed by two-dimensional scanning [35,39], where the residual error is  $<1$  nm rms. Trap stiffness was determined by standard methods [35,40]. Detailed methods and data analysis are described in Ref. [35].

Figure 1(b) shows single-molecule kinesin movement observed by using force-clamp optical tweezers with FPGA feedback. The apparatus automatically detects the kinesin walking and starts the force-clamp mode, which keeps the distance between the probe and the trap center constant. The trap center thus follows the probe motion that displays both thermal fluctuation and kinesin movement until the probe arrives at the end of the detectable range of the QPD. To obtain the response functions, we applied constant forces plus a sinusoidal perturbation of 1/5 times their magnitude [35].

Figure 2(a) shows a FRR of the probe movement at high ATP concentration (1 mM ATP, 0.1 mM ADP, 1 mM  $P_i$ ), which simulates physiological conditions where the input free energy change  $\Delta\mu = \Delta\mu^0 + k_B T \ln([ATP]/[ADP][P_i])$  is  $84.5 \pm 2.5$  pN nm [30,41–44]. Constant force was chosen as  $F_0 = -2$  pN, which simulates the condition for maximum output power [13]. The response,  $2k_B T \tilde{R}'(f)$ , and the fluctuation,  $\tilde{C}(f)$ , took almost the same values at high frequencies, but began to deviate once frequency fell below 20 Hz. This qualitative frequency dependence is

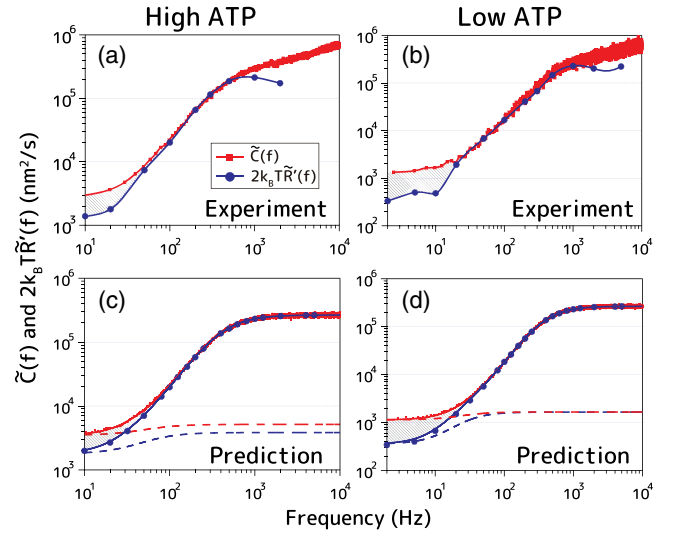


FIG. 2. (a) Typical examples of experimental results of FRR at high ATP (1 mM ATP, 0.1 mM ADP, 1 mM  $P_i$ ) and (b) low ATP (10  $\mu\text{M}$  ATP, 1  $\mu\text{M}$  ADP, 1 mM  $P_i$ ). *Square dots*: velocity fluctuations, *Circles*: response functions. *Lines* are cubic spline interpolations. (c) Model predictions of FRR at high ATP and (d) low ATP. *Dots and circles*: numerical simulations. *Lines* indicate analytical solutions. *Dashed lines* are analytical solutions from the kinesin motor. *Shaded areas* indicate violation of the FRR.

consistent with FRR violations reported in prior studies [27,30]. However, the experimental bandwidth of the FRR was limited [Fig. 2(a)] because of the small observation time period. The kinesin went out of detectable range in a few subseconds.

At low ATP concentration (10  $\mu\text{M}$  ATP, 1  $\mu\text{M}$  ADP, 1 mM  $P_i$ ), the kinesin velocity was reduced, while  $\Delta\mu$  was kept constant by maintaining the  $[ATP]/[ADP][P_i]$  ratio. In this condition, the spectrums were extended to lower frequencies so that violation of the FRR was observed [Fig. 2(b)]. The nonequilibrium dissipation rate corresponds to the integrated area of the deviation [Fig. 2(b), shaded area]. The dissipation via viscous drag and the output power against the external force are shown in Table I. The results show that both the nonequilibrium and viscous drag dissipation rates are smaller than the output power by over 1 order of magnitude.

The relationship between the input  $\Delta\mu$  per unit time, the output power, and the total heat dissipation rate is provided as

$$\Delta\mu/\tau = -F_0 \bar{v} + J_x + J_{\text{all others}}, \quad (2)$$

where  $J_{\text{all others}}$  is the heat dissipation rate via d.o.f. not observed here, and  $\tau$  is the turnover time for ATP hydrolysis by kinesin, which is estimated as  $\tau \approx d/\bar{v}$  since the frequency of backsteps at  $F_0 = -2$  pN is negligible. The experimental results indicate that the dissipation from

TABLE I. Summary of experimental results and model predictions for FRR.

Energy flows [pN nm/s]	High ATP			Low ATP		
	Experiment	Simulation	Solution	Experiment	Simulation	Solution
$-F_0 \bar{v}$	$1150 \pm 120$	$1110 \pm 20$	1070	$410 \pm 60$	$425 \pm 16$	410
$\gamma \bar{v}^2$	$10.6 \pm 1.9$	$9.58 \pm 0.34$	8.89	$1.35 \pm 0.37$	$1.40 \pm 0.11$	1.29
$2\gamma \int_0^{f_{\max}} df [\tilde{C}(f) - 2k_B T \tilde{R}'(\omega)]$	$53.4 \pm 41.4^a$	$27.2^b$	50.7	$2.74 \pm 1.52^a$	$1.83^b$	2.14
$J_x$	$63.9 \pm 41.5$	$62.5 \pm 6.2^c$	59.6	$4.09 \pm 1.56$	$4.53 \pm 3.19^c$	3.43
$\Delta\mu/\tau$	$6160 \pm 560^d$	$7000 \pm 226$	6820	$2190 \pm 310^d$	$2280 \pm 105$	2170

<sup>a</sup>Values were integrated up to  $f_{\max} = 300$  Hz for high ATP (mean  $\pm$  s.d.,  $n = 8$ ) and  $f_{\max} = 50$  Hz for low ATP ( $n = 11$ ).

<sup>b</sup>Values were integrated up to  $f_{\max} = 300$  Hz for high ATP and  $f_{\max} = 50$  Hz for low ATP.

<sup>c</sup>Values were directly calculated from the definition of  $J_x$  (mean  $\pm$  s.d.,  $n = 20$ ) [45].

<sup>d</sup>Values were estimated by using the approximation  $\tau \approx d/\bar{v}$ .

the probe's d.o.f. ( $J_x$ ) is dramatically smaller than the power. The sum of these values [the first two terms of the right-hand side of Eq. (2)] is  $\approx 20\%$  of the input,  $\Delta\mu$  (Table I), indicating that most ( $\approx 80\%$ ) of  $\Delta\mu$  is dissipated via other *hidden* d.o.f. ( $J_{\text{all others}}$ ).

Next we examine the origin of the hidden dissipation using a quantitative theoretical model. Existing mathematical models for kinesin movement fall into two classes. One mimics the kinesin movement using toy models such as thermal ratchets in which the kinesin tumbles on a (switching) one-dimensional potential [46–51]. To date, however, it was reported that when kinesin steps backward kinesin hydrolyzes ATP instead of synthesizing ATP [13–15], indicating that the backward step is not the reverse reaction of the forward one. Therefore, kinesin movement cannot be described by a one-dimensional potential [52]. Instead, kinesin is now believed to take multiple, branched kinetic pathways [17,52]. The other class adopts the Markov chain model to describe the discrete stochastic transitions in the network of kinetic states [23,53–56]. Although single-molecule observations and/or biochemical assays are used to extract the reaction rates between discrete states, most theoretical Markov models require experimentally inaccessible parameters.

Here, to investigate the kinesin movement without parameter tuning, we chose a phenomenological description that only uses experimentally accessible parameters. While abounding (Markov-like) kinetic diagrams have been proposed based on experimental observations [7,8,13,14,17,18,20,52], some intermediate (kinetic) parameters, especially for backsteps, are too rare or transient to determine experimentally [17]. We therefore adopted a simplified kinesin model in which the reaction process was reduced into two-state Markov transitions [14] [Fig. 3(a)]. In this model, the ATP hydrolysis cycle is composed of three transition paths (solid allows). One is load independent with rate constant  $k_c$  (state 1 to state 2), meaning that the reaction path is not coupled to any mechanical transitions (steps). The second and third paths are load dependent with  $k_f$  and  $k_b$  (state 2 to state 1) and are coupled to the mechanical transitions for forward and

backward steps, respectively. The load dependence of the transition rates are described by Bell's equation [57]:

$$k_f(F) = k_f^0 \exp\left(\frac{d_f F}{k_B T}\right), \quad (3)$$

$$k_b(F) = k_b^0 \exp\left(\frac{d_b F}{k_B T}\right), \quad (4)$$

where  $F$  is an external force (load),  $k_f^0$  and  $k_b^0$  are the rate constants at zero load, and  $d_f$  and  $d_b$  are the characteristic distances for forward and backward steps, respectively.

To satisfy thermodynamic consistency, local detailed balance [58–60] (constraints similar to microscopic reversibility [61,62] or steady-state balance [63]) conditions are required. For this purpose, three reverse paths are exhibited in the model [dashed allows in Fig. 3(a)]. Although small reverse rates for ATP synthesis by kinesin was measured by

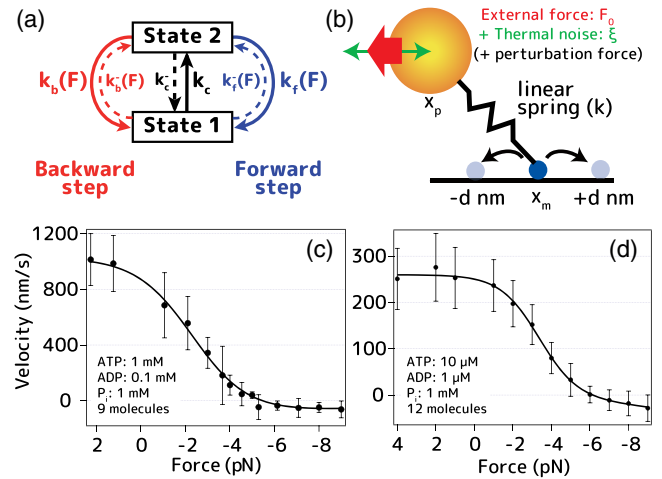


FIG. 3. (a) Schematic of a two-state kinesin stepper model. (b) Langevin model of a probe connected to the kinesin stepper. (c) Force-velocity relationship of single molecule kinesin movements at high ATP and (d) low ATP (mean  $\pm$  s.d.). Lines are fitted by Eq. (6). Fit parameters for high and low ATP are:  $k_f^0 = 981$  and  $889$ ,  $k_b^0 = 22.8$  and  $0.61$   $\text{s}^{-1}$ ,  $k_c = 129$  and  $32.5$   $\text{s}^{-1}$ ,  $d_f = 3.3$  and  $4.0$  nm, and  $d_b = 0.47$  and  $-0.83$  nm, respectively.

oxygen isotopic exchange [64], coupling with step movement have not been experimentally identified yet. Furthermore, in our experimental conditions at high  $\Delta\mu$ , the reverse rates ( $k_c^-$ ,  $k_f^-$ , and  $k_b^-$ ) are estimated to be negligibly small and barely affect the model predictions for FRR (data not shown). Thus, we use the simplified model that neglected these reverse transitions in the following analysis.

The observable in our experiment is the probe's position, which is pulled by the kinesin motor [Fig. 3(b)]. The motor is modeled as the Markov stepper that transits forward and backward with step size  $d$ , and the probe is connected with the motor via a linear spring of stiffness  $k$ . The probe's dynamics is described by an overdamped Langevin equation:

$$\gamma \frac{d}{dt} x_p = k(x_m - x_p) + F_0 + N_0 \sin 2\pi f t + \xi, \quad (5)$$

where  $x_m$  and  $x_p$  are the position of the motor and the probe, respectively,  $F_0$  is the external constant force,  $N_0$  is the magnitude of the sinusoidal perturbation force for response calculations with frequency  $f$ , and  $\xi$  is the thermal fluctuation force that satisfies  $\langle \xi \rangle = 0$  and  $\langle \xi(t)\xi(t') \rangle = 2k_B T \gamma \delta(t - t')$ .

Five parameters for the kinesin kinetic model,  $k_f^0$ ,  $k_b^0$ ,  $k_c$ ,  $d_f$ , and  $d_b$ , were obtained from the experimental results of the force-velocity relationship by fitting the theoretical equation derived from the model [Figs. 3(c) and 3(d); see Ref. [35] for deviation]:

$$\bar{v} = d \times \frac{(k_f - k_b)k_c}{k_f + k_b + k_c}, \quad (6)$$

where  $\bar{v}$  was the mean velocity, and  $d$  was the step size (8 nm) [3]. The stiffness  $k = 0.075$  pN/nm and viscous drag  $\gamma = 3.1 \times 10^{-5}$  pN/nm s were also obtained experimentally [35].

Analytical solutions for the fluctuation and the response of the model were derived [35] as

$$\tilde{C}(f) = \frac{k^2 \tilde{C}_m + 2k_B T \gamma (k \tilde{R}_m + i2\pi f)^2}{|k(1 + \gamma \tilde{R}_m) + i\gamma 2\pi f|^2}, \quad (7)$$

$$2k_B T \tilde{R}'(f) = \text{Re} \left( \frac{2k_B T (k \tilde{R}_m + i2\pi f)}{k(1 + \gamma \tilde{R}_m) + i\gamma 2\pi f} \right), \quad (8)$$

with  $\tilde{C}_m = d^2 k_c / k_a [(k_f + k_b) - 2(k_f - k_b)^2 k_c / (k_a^2 + 4\pi^2 f^2)]$ ,  $\tilde{R}_m = dk_c / k_a [(\alpha_f - \alpha_b) - (\alpha_f + \alpha_b)(k_f + k_b) / (k_a + i2\pi f)]$ ,  $k_a \equiv k_f + k_b + k_c$ ,  $\alpha_f \equiv k_f d_b / k_B T$ , and  $\alpha_b \equiv k_b d_b / k_B T$ . We confirmed the Harada-Sasa equality (1) holds for the model used here analytically by independently calculating the definition of  $J_x \equiv \langle (\gamma v - \xi) \circ v \rangle$  and the right-hand side of Eq. (1) [35]. Here, the circle indicates the Stratonovich product [45].

The FRRs obtained from the analytical solutions and numerical simulations are shown in Figs. 2(c) and 2(d) (lines and dots, respectively). The predicted FRRs similar to the experimental results [Figs. 2(a) and 2(b)] justify our analysis. The obtained dissipation rates, powers and input energy flows are shown in Table I. In addition,  $J_x$  was independently obtained by numerical simulations and the analytical solution. These values are similar to the experimentally obtained values, indicating that the model reproduces the experimental results.

Totally in contrast to the translational motor kinesin studied here, Toyabe *et al.* found that the sum of the work and the dissipations of the rotary motor F<sub>1</sub>-ATPase were almost the same as the input,  $\Delta\mu$ , indicating that the internal dissipation of the motor is negligible [30,31]. One candidate reason for the discrepancy is *reversibility*; F<sub>1</sub>-ATPase acts reversibly as a ‘‘power generator’’ that synthesizes ATP with backward rotation [65,66]. Theoretical models based on the reversibility could successfully explain the little internal dissipation [67,68]. Conversely, kinesin is irreversible and has multiple pathways that include futile ATP hydrolysis such as that for backsteps. The futile ATP hydrolysis *per se* should cause futile dissipation. However, at the experimental condition utilized here, the frequency of the backsteps is only a few percentage points. Although other slippage pathways are also conceivable, they are thought to be rare at conditions similar with this study [69]. This means that futile ATP hydrolysis mainly due to backsteps cannot account for the  $\approx 80\%$  hidden dissipation, at least under physiological conditions.

Another candidate reason is the softness of the linker between the probe and the motor. Because of the softness, the nonthermal fluctuation derived from the motor does not transmit to the probe efficiently at high frequencies, and the probe fluctuates merely thermally [27]. In the prior study using F<sub>1</sub>-ATPase [30,31], the duplex probe is directly connected to the rotary shaft so that the stiffness of the linker is considerably higher than that of kinesin. For kinesin, however, the probe is only loosely connected to the motor via its long stalk; the probe could not completely follow kinesin's rapid steps such that the observed dissipation ( $J_x$ ) might underestimate the actual dissipation from the kinesin movement. We therefore discuss the FRR of the kinesin motor separately from the probe, as explained below.

Dashed lines in Figs. 2(c) and 2(d) indicate the fluctuation and the response from the motor obtained using the analytical solution of the two-state Markov model ( $\tilde{C}_m$  and  $\tilde{R}'_m$ ; see Ref. [35] for derivations). At low frequencies, the FRR of the probe nearly agrees with the FRR of the motor, whereas violation of the FRR of the probe seems to attenuate over the cutoff frequency  $f_c = k/2\pi\gamma$ . Nevertheless, at low ATP, the FRR violation from the motor approximately agrees with that from the probe, indicating that the probe's FRR almost accurately reports

the dissipation from the motor despite the softness of the linker. Meanwhile, at high ATP, the FRR violation from the motor was observed even at the highest frequency. (Note that FRR at low ATP also shows small deviations at high frequencies.) The violation of FRR at the high frequency limit is given as  $\Delta = dk_c/k_a[k_f(d - 2d_f) + k_b(d + 2d_b)]$  [35,70]. This  $\Delta$  originates from the imbalance between the step size  $d$  and the characteristic distances  $d_f$  and  $d_b$ , which is thought to reflect the irreversibility of the system [71], a key element of nonequilibrium dynamics.

When the FRR is violated at high frequency limits, the nonequilibrium dissipation of the motor, which is estimated by integrating the violation towards infinite frequencies, should diverge. This thermodynamic inconsistency appears because the Markov step model assumes that kinesin moves at infinitely large velocity for each step, leading to infinite dissipation. However, the actual kinesin step requires finite time such that the cutoff frequency of the motor movement should exist. Recently, the motion of the kinesin head ( $\approx 5$  nm) was observed using a small gold particle at the rate of  $55 \mu\text{s}$  ( $\approx 18$  kHz), where the lag phase during a step could not be resolved [20]. This implies that the cutoff frequency is over tens of kHz and that the FRR violation of the actual motor decays beyond our observation frequencies. We thus made rough estimation of the cutoff frequency and evaluated the dissipation due to whole motor movement, but found we could not completely explain the  $\approx 80\%$  hidden dissipation [21,35].

By dismissing several candidate reasons, the hidden dissipation does not seem to occur through the translational motion of kinesin, but rather is consumed inside the kinesin molecule. The internal dissipation could be explained by introducing additional d.o.f. in the molecule, whereas our model considered only one observable, i.e., the kinesin position in discrete steps. Experimentally, direct observation of each head revealed the diffusion process, bound and unbound transitions, and off-axis movement of the head [20], suggesting that these microscopic mechanical transitions are required to elucidate the internal dissipations. In addition, the actual kinesin kinetics contains complicated reactions, including inherent *fast* transitions between microscopic structural states [72], whereas our kinesin model used here considered only *slow* transitions between coarse-grained states. Theoretically, these fast transitions can also contribute to heat dissipations [73,74]. Although the fast transitions neglected in our model mainly consist of intermediate transitions for ATP hydrolysis and they do not directly contribute to the translational motion [17,18,52], dissipations from the fast transitions might be required to achieve the biased unidirectional motion. In this case, multidimensional mathematical models including reaction coordinates [62,71] could also be suitable for clarifying the total energetics of kinesin.

In summary, we present the first experimental demonstration of violation of the FRR of a single-molecule

translational motor, kinesin. By using the Harada-Sasa equality, dissipative heat from the kinesin motor was measured *quantitatively*. The nonequilibrium dissipation via a probe attached to kinesin is dramatically small compared to the output power against external force. The sum of these energy rates is only  $\approx 20\%$  of the input, meaning that most ( $\approx 80\%$ ) chemical energy is consumed as hidden dissipations, which were not previously recognized. By analyzing the transmission of the motor action to probe fluctuations using a simplified kinesin model, we conclude that the hidden dissipation is “internal dissipation” of the motor. Recently, unobserved reaction pathways, hidden d.o.f., and their effects on the energetics of biomolecular machines have been intensively discussed [71,73–75]. By quantifying the internal dissipation of the kinesin molecule, our study will help clarify the unresolved nonequilibrium mechanism.

We acknowledge S.-i. Sasa, K. Kawaguchi, and S.-W. Wang for variable discussions, S. Toyabe for helping with data analyzing methods, and P. Karagiannis for critically revising the manuscript. This work was supported by JSPS KAKENHI JP25870173, JP15K05248, JP18K03564 (to T. A.), JP15H01494, JP15H03710, JP25127712, and JP25103011 (to D. M.).

\*ariga@yamaguchi-u.ac.jp

- [1] R. D. Vale, *Cell* **112**, 467 (2003).
- [2] N. Hirokawa, Y. Noda, Y. Tanaka, and S. Niwa, *Nat. Rev. Mol. Cell Biol.* **10**, 682 (2009).
- [3] K. Svoboda, C. F. Schmidt, B. J. Schnapp, and S. M. Block, *Nature (London)* **365**, 721 (1993).
- [4] M. J. Schnitzer and S. M. Block, *Nature (London)* **388**, 386 (1997).
- [5] W. Hua, E. C. Young, M. L. Fleming, and J. Gelles, *Nature (London)* **388**, 390 (1997).
- [6] K. Svoboda and S. M. Block, *Cell* **77**, 773 (1994).
- [7] H. Kojima, E. Muto, H. Higuchi, and T. Yanagida, *Biophys. J.* **73**, 2012 (1997).
- [8] K. Visscher, M. J. Schnitzer, and S. M. Block, *Nature (London)* **400**, 184 (1999).
- [9] K. Kaseda, H. Higuchi, and K. Hirose, *Nat. Cell Biol.* **5**, 1079 (2003).
- [10] C. L. Asbury, A. N. Fehr, and S. M. Block, *Science* **302**, 2130 (2003).
- [11] A. Yildiz, M. Tomishige, R. D. Vale, and P. R. Selvin, *Science* **303**, 676 (2004).
- [12] T. Mori, R. D. Vale, and M. Tomishige, *Nature (London)* **450**, 750 (2007).
- [13] M. Nishiyama, H. Higuchi, and T. Yanagida, *Nat. Cell Biol.* **4**, 790 (2002).
- [14] Y. Taniguchi, M. Nishiyama, Y. Ishii, and T. Yanagida, *Nat. Chem. Biol.* **1**, 342 (2005).
- [15] N. J. Carter and R. A. Cross, *Nature (London)* **435**, 308 (2005).
- [16] A. Yildiz, M. Tomishige, A. Gennerich, and R. D. Vale, *Cell* **134**, 1030 (2008).

- [17] B. E. Clancy, W. M. Behnke-Parks, J. O. Andreasson, S. S. Rosenfeld, and S. M. Block, *Nat. Struct. Mol. Biol.* **18**, 1020 (2011).
- [18] B. Milic, J. O. Andreasson, W. O. Hancock, and S. M. Block, *Proc. Natl. Acad. Sci. U.S.A.* **111**, 14136 (2014).
- [19] M. Y. Dogan, S. Can, F. B. Cleary, V. Purde, and A. Yildiz, *Cell Rep.* **10**, 1967 (2015).
- [20] H. Isojima, R. Iino, Y. Niitani, H. Noji, and M. Tomishige, *Nat. Chem. Biol.* **12**, 290 (2016).
- [21] J. Howard, *Mechanics of Motor Proteins and the Cytoskeleton* (Sinauer Associates, Inc., Sunderland, 2001).
- [22] S. Toyabe, T. Watanabe-Nakayama, T. Okamoto, S. Kudo, and E. Muneyuki, *Proc. Natl. Acad. Sci. U.S.A.* **108**, 17951 (2011).
- [23] A. B. Kolomeisky and M. E. Fisher, *Annu. Rev. Phys. Chem.* **58**, 675 (2007).
- [24] T. Harada and S.-i. Sasa, *Phys. Rev. Lett.* **95**, 130602 (2005).
- [25] T. Harada and S.-i. Sasa, *Phys. Rev. E* **73**, 026131 (2006).
- [26] R. Kubo, M. Toda, and N. Hashitsume, *Statistical Physics II: Nonequilibrium Statistical Mechanics* (Springer-Verlag, Berlin, 1991).
- [27] D. Mizuno, C. Tardin, C. F. Schmidt, and F. C. MacKintosh, *Science* **315**, 370 (2007).
- [28] K. Nishizawa, M. Bremerich, H. Ayade, C. F. Schmidt, T. Ariga, and D. Mizuno, *Sci. Adv.* **3**, e1700318 (2017).
- [29] S. Toyabe, H.-R. Jiang, T. Nakamura, Y. Murayama, and M. Sano, *Phys. Rev. E* **75**, 011122 (2007).
- [30] S. Toyabe, T. Okamoto, T. Watanabe-Nakayama, H. Taketani, S. Kudo, and E. Muneyuki, *Phys. Rev. Lett.* **104**, 198103 (2010).
- [31] S. Toyabe and E. Muneyuki, *New J. Phys.* **17**, 015008 (2015).
- [32] É. Fodor, W. W. Ahmed, M. Almonacid, M. Bussonnier, N. S. Gov, M.-H. Verlhac, T. Betz, P. Visco, and F. van Wijland, *Europhys. Lett.* **116**, 30008 (2016).
- [33] K. C. Neuman and S. M. Block, *Rev. Sci. Instrum.* **75**, 2787 (2004).
- [34] N. Uchida, K. Okuro, Y. Niitani, X. Ling, T. Ariga, M. Tomishige, and T. Aida, *J. Am. Chem. Soc.* **135**, 4684 (2013).
- [35] See Supplemental Material at <http://link.aps.org/supplemental/10.1103/PhysRevLett.121.218101> for detailed materials and methods, data analysis procedures, deviations for analytical solutions, and supplementary discussions.
- [36] T. Aoki, M. Tomishige, and T. Ariga, *Biophysics* **9**, 149 (2013).
- [37] G. T. Hermanson, *Bioconjugate Techniques*, 2nd ed. (Academic Press, New York, 2008) p. 598.
- [38] T. Mitchison and M. Kirschner, *Nature (London)* **312**, 232 (1984).
- [39] M. J. Lang, C. L. Asbury, J. W. Shaevitz, and S. M. Block, *Biophys. J.* **83**, 491 (2002).
- [40] F. Gittes and C. F. Schmidt, *Methods Cell Biol.* **55**, 129 (1997).
- [41] K. Krab and J. Van Wezel, *Biochim. Biophys. Acta* **1098**, 172 (1992).
- [42] J. Rosing and E. Slater, *Biochim. Biophys. Acta* **267**, 275 (1972).
- [43] R. W. Guynn and R. L. Veech, *J. Biol. Chem.* **248**, 6966 (1973).
- [44] O. Pänke and B. Rumberg, *Biochim. Biophys. Acta* **1322**, 183 (1997).
- [45] K. Sekimoto, *J. Phys. Soc. Jpn.* **66**, 1234 (1997).
- [46] R. D. Vale and F. Oosawa, *Adv. Biophys.* **26**, 97 (1990).
- [47] N. J. Córdova, B. Ermentrout, and G. F. Oster, *Proc. Natl. Acad. Sci. U.S.A.* **89**, 339 (1992).
- [48] M. O. Magnasco, *Phys. Rev. Lett.* **71**, 1477 (1993).
- [49] R. D. Astumian and M. Bier, *Phys. Rev. Lett.* **72**, 1766 (1994).
- [50] J. Prost, J.-F. Chauwin, L. Peliti, and A. Ajdari, *Phys. Rev. Lett.* **72**, 2652 (1994).
- [51] C. S. Peskin and G. Oster, *Biophys. J.* **68**, 202S (1995).
- [52] C. Hyeon, S. Klumpp, and J. N. Onuchic, *Phys. Chem. Chem. Phys.* **11**, 4899 (2009).
- [53] S. Leibler and D. A. Huse, *J. Cell Biol.* **121**, 1357 (1993).
- [54] M. E. Fisher and A. B. Kolomeisky, *Proc. Natl. Acad. Sci. U.S.A.* **96**, 6597 (1999).
- [55] C. Maes and M. H. Van Wieren, *J. Stat. Phys.* **112**, 329 (2003).
- [56] S. Liepelt and R. Lipowsky, *Phys. Rev. Lett.* **98**, 258102 (2007).
- [57] G. I. Bell, *Science* **200**, 618 (1978).
- [58] T. L. Hill, *Free Energy Transduction and Biochemical Cycle Kinetics* (Dover Publications, New York, 1989).
- [59] U. Seifert, *Eur. Phys. J. E* **34**, 26 (2011).
- [60] E. Zimmermann and U. Seifert, *Phys. Rev. E* **91**, 022709 (2015).
- [61] R. D. Astumian, *Nat. Nanotechnol.* **7**, 684 (2012).
- [62] R. D. Astumian, S. Mukherjee, and A. Warshel, *ChemPhys-Chem* **17**, 1719 (2016).
- [63] S. Liepelt and R. Lipowsky, *Europhys. Lett.* **77**, 50002 (2007).
- [64] D. D. Hackney, *Proc. Natl. Acad. Sci. U.S.A.* **102**, 18338 (2005).
- [65] H. Itoh, A. Takahashi, K. Adachi, H. Noji, R. Yasuda, M. Yoshida, and K. Kinosita Jr., *Nature (London)* **427**, 465 (2004).
- [66] Y. Rondelez, G. Tresset, T. Nakashima, Y. Kato-Yamada, H. Fujita, S. Takeuchi, and H. Noji, *Nature (London)* **433**, 773 (2005).
- [67] E. Zimmermann and U. Seifert, *New J. Phys.* **14**, 103023 (2012).
- [68] K. Kawaguchi, S.-i. Sasa, and T. Sagawa, *Biophys. J.* **106**, 2450 (2014).
- [69] T. Sumi, *Sci. Rep.* **7**, 1163 (2017).
- [70] S.-W. Wang, *Phys. Rev. E* **97**, 052125 (2018).
- [71] T. Harada and N. Nakagawa, *Europhys. Lett.* **78**, 50002 (2007).
- [72] R. Cross, *Biopolymers* **105**, 476 (2016).
- [73] S.-W. Wang, K. Kawaguchi, S.-i. Sasa, and L.-H. Tang, *Phys. Rev. Lett.* **117**, 070601 (2016).
- [74] S.-W. Wang, K. Kawaguchi, S.-i. Sasa, and L.-H. Tang, [arXiv:1610.00120](https://arxiv.org/abs/1610.00120).
- [75] N. Shiraishi and T. Sagawa, *Phys. Rev. E* **91**, 012130 (2015).